Aust. J. Phys., 1982, **35**, 571–91

Electron Coincidence Spectroscopy: An Introduction to Momentum Space Chemistry

Erich Weigold

School of Physical Sciences, Flinders University of South Australia, Bedford Park, S.A. 5042.

Abstract

The application of electron coincidence or (e, 2e) spectroscopy to obtaining detailed information on the dynamic structure of atoms and molecules is discussed. The technique obtains separation energy spectra and spherically averaged electron momentum distributions for each molecular orbital in the valence region. A brief discussion of molecular orbital density functions in momentum space is given. The results using Hartree–Fock wavefunctions for atomic orbitals and LCAO–MO wavefunctions for molecular orbitals are compared with (e, 2e) data. The sensitivity of the data to electron correlations in either the initial or final ion many body states is discussed and examples are given.

1. Introduction

The dynamic electronic structure of atoms and molecules can be directly observed by means of the (e, 2e) reaction, which measures the distribution of energies and momenta of two electrons in coincidence after a knockout reaction initiated by an electron beam of known momentum incident on an atomic or molecular gas target. Basically in an (e, 2e) reaction the incident electron of energy E_0 and momentum $\boldsymbol{p}_0$ ionizes the N electron target (which is usually in its ground state Ψ_0^N), producing an ion in a state Ψ_F^{N-1} and two free electrons of energies and momenta $E_A, \boldsymbol{p}_A$ and $E_B, \boldsymbol{p}_B$. The outgoing electrons are emitted at angles θ_A, ϕ_A and θ_B, ϕ_B, where the z direction is the direction of the incident electron. From energy and momentum conservation, the electron separation energy leading to the ion eigenstate Ψ_F^{N-1} is given simply by

$$\varepsilon_F = E_0 - E_A - E_B, \tag{1}$$

and the recoil momentum $\boldsymbol{q}$ of the ion is

$$\boldsymbol{q} = \boldsymbol{p}_0 - \boldsymbol{p}_A - \boldsymbol{p}_B. \tag{2}$$

At high enough energies the electron waves can be well approximated by plane waves, and then if the ejected electron is knocked cleanly out of the target system by the scattered electron, the momentum $\boldsymbol{p}$ of the ejected electron prior to the collision is given simply by

$$\boldsymbol{p} = -\boldsymbol{q}. \tag{3}$$

The kinematical conditions under which one obtains a clean knockout of an electron from the target system have been extensively discussed by McCarthy and Weigold (1976), Weigold and McCarthy (1978) and Weigold (1981). Briefly, in order to

obtain close electron–electron collisions one chooses the kinematics so that the momentum $\boldsymbol{K}$ transferred between the incident electron and the target is maximized. By convention one usually calls the 'scattered' electron the faster outgoing electron, so that

$$\boldsymbol{K} = \boldsymbol{p}_0 - \boldsymbol{p}_A, \tag{4}$$

where $p_A \geqslant p_B$.

Since electrons are indistinguishable, the condition for maximum K requires that $K = |\boldsymbol{p}_0 - \boldsymbol{p}_A| = |\boldsymbol{p}_0 - \boldsymbol{p}_B|$, i.e. $p_A = p_B$, $E_A = E_B$ and $\theta_A = \theta_B = \theta$. This is called symmetric kinematics. For free electron collisions where the struck electron is initially at rest ($p = 0$), $\theta = 45°$ and the out-of-plane azimuthal angle $\phi = \pi - (\phi_A - \phi_B)$ must be zero. For struck electrons which are not initially at rest the outgoing angles will differ from $\phi = 0$ and $\theta = 45°$. The geometry in which $\phi = 0$ and θ is varied is called the coplanar symmetric geometry. If θ is kept fixed (at approximately 45°) and ϕ is varied we have the non-coplanar symmetric geometry. For structure determination non-coplanar symmetric kinematics are preferred (see McCarthy and Weigold 1976).

It is obvious that the symmetric (e, 2e) cross section at any θ and ϕ will depend on the probability of the struck electron having the corresponding momentum $\boldsymbol{p} = \boldsymbol{p}_A + \boldsymbol{p}_B - \boldsymbol{p}_0$. In electron coincidence spectroscopy two types of measurements are made. Firstly, the (e, 2e) cross section is measured as a function of the incident energy for fixed E_A ($= E_B$), θ and ϕ. This gives an electron separation energy spectrum at essentially fixed p (see equation 1). Secondly, at energies corresponding to a separation energy peak, the cross section is measured as a function of p, i.e. as a function of ϕ in the non-coplanar symmetric geometry. The angular correlation measurement yields a momentum profile since

$$p = \{(2p_A \cos\theta - p_0)^2 + 4p_A^2 \sin^2\theta \sin^2\tfrac{1}{2}\phi\}^{\frac{1}{2}}. \tag{5}$$

In order to extract detailed information on the dynamic structure of the target we must have an accurate theory to describe the reaction. At high electron energies and for symmetric kinematics such a theory is the plane wave impulse approximation (PWIA).

2. The (e, 2e) Cross Section

If we make the independent particle or Hartree–Fock (HF) approximation for the target, we can think of the target being composed of N electrons moving independently of each other in a self-consistent potential, each electron being in its characteristic orbital and having a characteristic (orbital) binding or separation energy. The (e, 2e) cross section $\sigma(\boldsymbol{p}_0, \boldsymbol{p}_A, \boldsymbol{p}_B)$ for an electron with separation energy $\varepsilon_F = E_0 - E_A - E_B$ can then be thought of as being the product of two factors. First we have the factor which describes the electron–electron collision probability. If we ignore the relatively small binding energy of the electron (i.e. $E_A, E_B \gg \varepsilon_F$), the distribution of final momenta in a two-electron collision is simply given by the Rutherford cross section, which is given by (in a.u.)

$$f_{ee}(\boldsymbol{p}_0, \boldsymbol{p}_A, \boldsymbol{p}_B) = 4|\boldsymbol{p}_0 - \boldsymbol{p}_A|^{-4} = 4K^{-4}. \tag{6}$$

The second factor is the probability of the electron having momentum $\boldsymbol{p} = \boldsymbol{p}_A + \boldsymbol{p}_B - \boldsymbol{p}_0$ when struck. In the independent particle model this is simply the square of the electron momentum space wavefunction $|\phi_c(\boldsymbol{p})|^2$, where the subscript c indicates that it is the characteristic orbital of the electron. Therefore the 'classical' (e, 2e) cross section is given simply by

$$\sigma(\boldsymbol{p}_0, \boldsymbol{p}_A, \boldsymbol{p}_B) = 4K^{-4} |\phi_c(\boldsymbol{p})|^2 . \tag{7}$$

Note that for non-coplanar symmetric kinematics with fixed E_0 and E_A $(=E_B)$, K is constant and therefore the cross section (angular correlation) is directly proportional to $|\phi_c(\boldsymbol{p})|^2$.

The Rutherford electron–electron collision cross section makes no allowance for the indistinguishability of the two electrons. The corrections allowing for this were introduced by Mott, and these must be included in a more accurate expression for the cross section. Similarly, we have not allowed for the fact that the struck electron is initially bound and not free.

In general the differential cross section is (McCarthy and Weigold 1976)

$$\sigma_F(\boldsymbol{p}_0, \boldsymbol{p}_A, \boldsymbol{p}_B) = (2\pi)^4 \sum_{av} \frac{p_A p_B}{p_0} |M_F(\boldsymbol{p}_0, \boldsymbol{p}_A, \boldsymbol{p}_B)|^2 , \tag{8}$$

where Σ_{av} denotes the average over initial and the sum over final degeneracies. At high enough energies the electron waves may be treated as plane waves $(|\boldsymbol{p}\rangle = (2\pi)^{-3/2} \exp(i\boldsymbol{p}.\boldsymbol{r}))$ and the (e, 2e) amplitude may be written as

$$M_F(\boldsymbol{p}_0, \boldsymbol{p}_A, \boldsymbol{p}_B) = \mathsf{A} \langle \boldsymbol{p}_A, \boldsymbol{p}_B \Psi_F^{N-1} | T(E) | \Psi_0^N \boldsymbol{p}_0 \rangle . \tag{9}$$

The operator A indicates that antisymmetrization must be performed over the coordinates of all the electrons and the bracket notation indicates that the integral is over these coordinates. The wavefunctions of the initial and final systems are connected by the transition operator $T(E)$, where the total energy is $E = E_A + E_B = E_0 - \varepsilon_F$.

If we assume the direct knockout of the electron, T must be a three body operator, depending only on the coordinates of the two colliding electrons and the centre of mass of the residual ion. Then Ψ_F^{N-1} commutes with T since it does not depend on the coordinates of the colliding electrons. To a good approximation $T(E)$ can be replaced by the antisymmetrized electron–electron collision amplitude (Weigold and McCarthy 1978), and the differential cross section is given by

$$\sigma_F = (2\pi)^4 \frac{p_A p_B}{p_0} f_{ee} \sum_{av} |\langle \boldsymbol{p} \Psi_F^{N-1} | \Psi_0^N \rangle|^2 , \tag{10}$$

where f_{ee} is simply the Mott electron–electron scattering factor at the total energy $E = E_0 - \varepsilon_F$, and the structure factor $\langle \boldsymbol{p} \Psi_F^{N-1} | \Psi_0^N \rangle$ is the momentum representation of the overlap amplitude for the target and ion eigenstates. This amplitude involves the integration over the coordinates of the $N-1$ common electrons of the product of the target and final ion momentum space wavefunctions, and is therefore a function only of the momentum of the ejected electron.

In symmetric kinematics, where $|\boldsymbol{p}_0-\boldsymbol{p}_A| = |\boldsymbol{p}_0-\boldsymbol{p}_B| = K$, the electron scattering factor takes the particularly simple analytic form (McCarthy and Weigold 1976)

$$f_{ee} = \frac{1}{4\pi^4}\frac{2\pi\eta}{\exp(2\pi\eta)-1}\frac{1}{K^4}, \tag{11}$$

where the factor involving $\eta = |\boldsymbol{p}_A-\boldsymbol{p}_B|^{-1}$ is the Gamow factor which determines the particle density in Coulomb scattering. At high energies η is very small and essentially constant and the Gamow factor is approximately unity. The high energy symmetric (e, 2e) cross section is therefore given by

$$\sigma_F(\boldsymbol{p}_0,\boldsymbol{p}_A,\boldsymbol{p}_B) = \frac{4}{K^4}\frac{p_A p_B}{p_0}\frac{2\pi\eta}{\exp(2\pi\eta)-1}\sum_{av}|\langle \boldsymbol{p}\,\Psi_F^{N-1}|\,\Psi_0^N\rangle|^2$$

$$\approx \frac{4}{K^4}\frac{p_A p_B}{p_0}\sum_{av}|\langle \boldsymbol{p}\Psi_F^{N-1}|\,\Psi_0^N\rangle|^2, \tag{12}$$

and the similarity to the simple classical expression (7) is striking, especially when the overlap between the target and ion wavefunctions is given by the single particle wavefunction $\psi_c(\boldsymbol{p})$ to a good approximation.

For singlet molecular targets, i.e. closed shell targets, the degeneracy of the structure factor arises from the fact that the initial (ground) electronic and vibrational state has a thermal distribution of rotational states and that the final rotational and vibrational states are usually not resolved. On making the Born–Oppenheimer approximation, the differential cross section (10) reduces to (McCarthy and Weigold 1976)

$$\sigma_F = (2\pi)^4\frac{p_A p_B}{p_0}f_{ee}\,n_r\int d\Omega\int dv\,|\langle \boldsymbol{p}\Psi_F^{N-1}|\,\Psi_0^N\rangle|^2. \tag{13}$$

The factor n_r comes from the sum over degenerate final states, there being n_r equivalent electrons in representation r. Thus the cross section is proportional to the spherically (i.e. rotationally) and vibrationally averaged square of the momentum space electronic overlap function. The vibrational average can be accurately approximated by calculating the overlap function at the equilibrium nuclear positions, reducing equation (13) to

$$\sigma_F = (2\pi)^4\frac{p_A p_B}{p_0}f_{ee}\,n_r\int d\Omega\,|\langle \boldsymbol{p}\Psi_F^{N-1}|\,\Psi_0^N\rangle|^2. \tag{14}$$

In the case of atoms the rotational integral in equation (13) can be readily performed, and we need consider only the overlap of radial functions.

3. Overlap Amplitude

The overlap amplitude may be computed directly from the one particle Green function describing the sudden ionization of an N particle system (Dixon *et al.* 1977; Williams *et al.* 1977). The poles of the Green function give the energies of the ion states excited in the transition and the pole strengths (or spectroscopic factors) give the relative intensities. In the independent particle picture and ignoring relaxation

of the core (i.e. the different self-consistent fields for the N and $N-1$ particle systems), only one ion eigenstate would be excited for an electron knocked out of its characteristic orbital. The pole strength for that ion eigenstate would be unity and for all other ion states belonging to that representation the pole strength would be zero. In general, electron correlations can lead to many ion states being excited with pole strengths ranging from 0 to 1. The higher the pole strength the better is the independent particle model for the transition.

Configuration Interaction Picture

The overlap function is perhaps more easily understood in terms of configuration interaction (CI) expansions of the states Ψ_F^{N-1} and Ψ_0^N, assuming that the ion states are bound states or narrow resonances. Expanding each many electron function in terms of HF functions Φ_α of the target, we have quite generally

$$\Psi_0^N = \sum_\alpha a_\alpha \Phi_\alpha, \qquad \Psi_F^{N-1} = \sum_{j\beta} t_{j\beta}^{(F)} C_{jr\beta} \psi_j^\dagger \Phi_\beta, \tag{15a, b}$$

where $\psi_j^\dagger$ is a hole in the single particle orbital j coupled to a target HF configuration Φ_β by a Clebsch–Gordan coefficient, which ensures that the configuration belongs to the particular representation r of the point group of the target.

The normalized antisymmetrized overlap amplitude is given by

$$\langle \boldsymbol{p}\Psi_F^{N-1} \mid \Psi_0^N \rangle = n_r^{\frac{1}{2}} \sum_{j\alpha} a_\alpha t_{j\alpha}^{(F)} C_{jr\alpha} \phi_j(\boldsymbol{p}), \tag{16}$$

where $\phi_j(\boldsymbol{p})$ is the momentum space single particle orbital wavefunction of the electron in the single particle orbital j. This expression is quite general and includes 'relaxation' effects as well as electron correlation effects.

Target HF Approximation

In the special case when the target state Ψ_0^N can be accurately described by the HF ground state Φ_0, then $a_\alpha = 0$ for $\alpha \neq 0$ and we have configuration interaction only in the final states (FSCI) and relaxation effects:

$$\langle \boldsymbol{p}\Psi_F^{N-1} \mid \Psi_0^N \rangle = n_r^{\frac{1}{2}} \sum_j t_{j0}^{(F)} C_{jr0} \phi_j(\boldsymbol{p}). \tag{17}$$

For atoms there is only one term $j = \mathrm{c}$ in the sum over j (i.e. the characteristic orbital of the electron). This is also often true for molecules; there may however sometimes be interactions between hole states, such as the 3σ and 4σ orbitals. For atoms (and most molecular cases) the characteristic orbital c of the representation r is defined by

$$\langle \boldsymbol{p}\Psi_F^{N-1} \mid \Psi_0^N \rangle = t_{\mathrm{c}0}^{(F)} \phi_{\mathrm{c}}(\boldsymbol{p}). \tag{18}$$

(The Clebsch–Gordan coefficient C_{jr0} is equal to $n_r^{-\frac{1}{2}}$.) The (e, 2e) cross section is therefore

$$\sigma_F = (2\pi)^4 \frac{p_\mathrm{A} p_\mathrm{B}}{p_0} f_{\mathrm{ee}} n_r \mid t_{\mathrm{c}0}^F \mid^2 \int \mathrm{d}\Omega \mid \phi_{\mathrm{c}}(\boldsymbol{p}) \mid^2. \tag{19}$$

In the non-coplanar symmetric geometry where f_{ee} is essentially constant, the (e, 2e) cross section is directly proportional to the square of the momentum space wave-

function of the characteristic orbital from which the electron is ejected. The strength of the transition is proportional to the spectroscopic factor (pole strength) $S_c^{(F)} = |t_{c0}^{(F)}|^2$. From closure and normalization one obtains the spectroscopic sum rule for the point group representation r

$$\sum_F S_c^{(F)} = 1, \quad F \in r. \tag{20}$$

Ground State Correlations

If there are electron correlation effects in the target ground state, nonzero contributions for orbitals $j \neq c$ will arise. These are generally very small since each contribution has a factor $(a_\alpha t_{j\alpha}^{(F)} C_{jr\alpha})^2$, which is very small because each coefficient in the factor is moderately small. However, such effects can sometimes be important. Firstly, for instance, in a restricted region of momentum space $|\psi_j(\boldsymbol{p})|^2$ may be very much greater than $|\psi_c(\boldsymbol{p})|^2$. Secondly, initial state configuration interaction (ISCI) can lead to the excitation of final ion states which are strictly forbidden in the target HF approximation. In this case the large coefficient a_0 does not contribute and the cross sections for such states F are sensitive to small coefficients a_α, $\alpha \neq 0$. We shall see an example later in the excitation of the $n = 2$ levels of He^+.

4. Orbitals in Momentum Space

The general CI expression (16) for the overlap amplitude yields an expression for the (e, 2e) cross section which involves a sum over the square of single particle momentum space orbitals. In the case where CI can be ignored in the ground state, this sum reduces (in nearly all cases) to a single orbital, the characteristic orbital from which the electron is ejected. The Schrödinger equation for a many body atomic or molecular system is usually solved in configuration space, and we are all used to thinking of the approximate single particle orbitals in this space. The momentum and position state functions are of course related by the Dirac–Fourier transformation and the complete knowledge of one implies a complete knowledge of the other:

$$\phi_j(\boldsymbol{p}) = (2\pi)^{-3/2} \int \mathrm{d}\boldsymbol{r}\, \psi_j(\boldsymbol{r}) \exp(-\mathrm{i}\boldsymbol{p}\cdot\boldsymbol{r}). \tag{21}$$

To construct the Schrödinger equation in momentum space from the classical Hamiltonian we must Fourier transform $V(\boldsymbol{r}_1, \ldots, \boldsymbol{r}_N)\, \Psi(\boldsymbol{r}_1, \ldots, \boldsymbol{r}_N)$ to obtain the potential energy operator in momentum representation, giving us an integral rather than the more normal differential equation. The solution of this equation is usually regarded as being difficult, and the relation (21) is usually used to obtain the momentum representation from the position space wavefunction. However, in atomic and molecular systems the essential interaction is the $|r|^{-1}$ Coulomb interaction, whose Fourier transform is simply $(2\pi^2 |\boldsymbol{p}|^2)^{-1}$, and it is easy to write the Schrödinger equation in momentum space. Indeed one simplification for a many body system is that multicentre singularities in position space are translated to the origin in momentum space.

The shapes of momentum space wavefunctions form an interesting study, which was first undertaken by Coulson and co-workers (Duncanson and Coulson 1941 and references therein). In order to compare them with present (e, 2e) measurements on gaseous targets we must spherically average the calculated momentum distributions, with unfortunately a resultant loss in some of the detailed shape information. However, a great deal of information remains even after the spherical averaging.

Atomic single particle wavefunctions can be expressed as the product of a radial wavefunction $R_{nl}(r)$ and a spherical harmonic $Y_{lm}(\hat{\boldsymbol{r}})$:

$$\psi_{nlm}(\boldsymbol{r}) = R_{nl}(r)\,Y_{lm}(\hat{\boldsymbol{r}}). \tag{22}$$

Taking the Fourier transform (21) we obtain

$$\phi_{nlm}(\boldsymbol{p}) = P_{nlm}(p)\,Y_{lm}(\hat{\boldsymbol{p}}), \tag{23}$$

where

$$P_{nl}(p) = (2/\pi)^{\frac{1}{2}}(-\mathrm{i})^l \int r^2\,\mathrm{d}r\,\mathrm{j}_l(pr)\,R_{nl}(r),$$

and $\mathrm{j}_l(pr)$ is the spherical Bessel function. The wavefunction in both spaces has the identical angular form Y_{lm}. The radial forms are rather similar and therefore atomic charge and momentum density maps, which are contour maps of the squares of the corresponding wavefunctions, are rather similar.

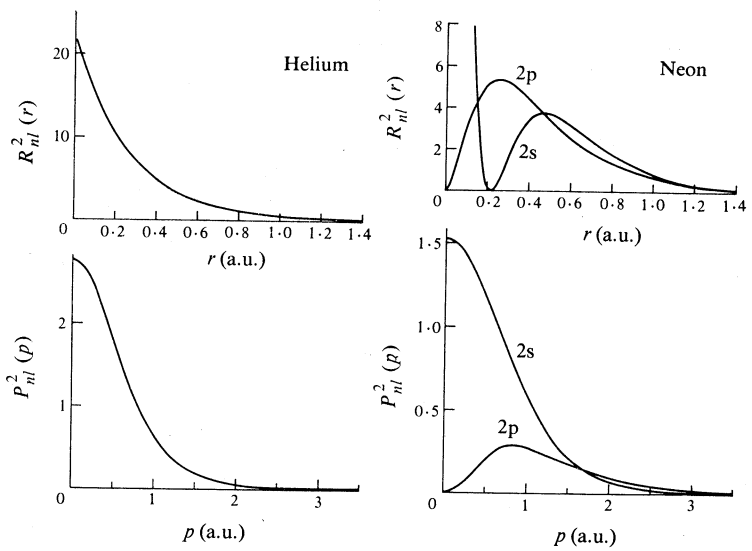

Fig. 1. Spherically averaged position and momentum probability distributions for 1s electrons in helium and the valence 2s and 2p electrons in neon using the HF wavefunctions of Clementi and Roetti (1974).

On spherical averaging the absolute squares of the wavefunctions, we are left with only the radial part of the charge and momentum densities $R_{nl}^2(r)$ and $P_{nl}^2(p)$. These are illustrated in Fig. 1 for the 1s electrons of helium and the valence 2s and 2p electrons of neon, using the HF wavefunctions of Clementi and Roetti (1974).

The situation for molecules can best be demonstrated by using a multicentre linear combination of atomic orbitals (LCAO) to approximate the single particle wavefunction. The independent particle (orbital) wavefunctions are obtained by approximate solutions of the HF equations for the molecule. The 'atomic' functions have particular angular properties centred on the nuclei, the nuclear positions determining the symmetry of the orbital.

Only two types of atomic functions A_μ are needed to specify the symmetry of a molecular orbital (MO). They are a spherically symmetric function called S and a vector function called $\boldsymbol{P}$, whose components P_x, P_y and P_z are related to the spherical harmonics Y_{lm}.

In terms of the distance r_s and direction θ_s, ϕ_s of the electron from the atomic centre $\boldsymbol{R}_s$, these symmetry functions A_μ are defined by

$$A_0 = S = (4\pi)^{\frac{1}{2}} Y_{00}(\theta_s, \phi_s) = 1, \tag{24a}$$

$$A_x = P_x = r_s(\tfrac{4}{6}\pi)^{\frac{1}{2}}\{Y_{1-1}(\theta_s, \phi_s) - Y_{11}(\theta_s, \phi_s)\} = r_s \sin\theta_s \cos\phi_s, \tag{24b}$$

$$A_y = P_y = r_s(\tfrac{4}{6}\pi)^{\frac{1}{2}} i\{Y_{1-1}(\theta_s, \phi_s) + Y_{11}(\theta_s, \phi_s)\} = r_s \sin\theta_s \sin\phi_s, \tag{24c}$$

$$A_z = P_z = r_s(\tfrac{4}{3}\pi)^{\frac{1}{2}} Y_{10}(\theta_s, \phi_s) = r_s \cos\theta_s. \tag{24d}$$

Each 'atomic' orbital (AO) $\psi_i^{(s)}(\boldsymbol{r}_s)$ in the linear combination consists of a product of a symmetry function with a radial function $u_\mu^s(r_s)$ centred at $\boldsymbol{R}_s$:

$$\psi_i^{(s)}(\boldsymbol{r}_s) = \sum_\mu u_\mu^s(r_s) A_\mu(\boldsymbol{r}_s), \tag{25}$$

and the LCAO is therefore given by

$$\psi_i(\boldsymbol{r}) = \sum_s \psi_i^{(s)}(\boldsymbol{r} - \boldsymbol{R}_s).$$

For ease of calculation the radial functions $u_\mu^{(s)}(r_s)$ are parametrized as a linear combination of gaussians $\exp(-\zeta r^2)$, where the exponents ζ span the range appropriate to the particular molecule. We get

$$\begin{aligned}\phi_i(\boldsymbol{p}) &= (2\pi)^{-3/2} \int \mathrm{d}^3 r \exp(-i\boldsymbol{p}.\boldsymbol{r}) \psi_i(\boldsymbol{r}) \\ &= (2\pi)^{-3/2} \sum_s \int \mathrm{d}^3 r \exp(-i\boldsymbol{p}.\boldsymbol{r}) \psi_i^{(s)}(\boldsymbol{r} - \boldsymbol{R}_s) \\ &= \sum_s \phi_i^s(\boldsymbol{p}) \exp(-i\boldsymbol{p}.\boldsymbol{R}_s),\end{aligned} \tag{26}$$

where the momentum space AO for atomic centre $\boldsymbol{R}_s$ is

$$\begin{aligned}\phi_i^{(s)}(\boldsymbol{p}) &= (2\pi)^{-3/2} \int \mathrm{d}^3 r \exp(-i\boldsymbol{p}.\boldsymbol{r}) \psi_i^{(s)}(\boldsymbol{r}) \\ &= \sum_\mu V_\mu^{(s)}(p) A_\mu(\boldsymbol{p}),\end{aligned} \tag{27}$$

and where as a result of the properties of the spherical harmonics Y_{lm} of which A_μ is a linear combination, the symmetry function again transforms into the same function of electron momentum $\boldsymbol{p}$. The radial function is

$$p^l V_\mu^{(s)}(p) = |2/\pi|^{\frac{1}{2}} i^l \int \mathrm{d}r\, r^{l+2} j_l(pr) u_\mu^{(s)}(r),$$

where $l = 0$ for S and $l = 1$ for $\boldsymbol{P}$.

In momentum space all the AO are centred at the origin of momentum. In momentum space the information about the atomic centres appears in the phase factors $\exp(-i\boldsymbol{p}.\boldsymbol{R}_s)$ in the linear combination (26). These phases have a small effect for $p \ll 1/R_{st}$, where R_{st} is the distance between atoms s and t.

As an example we can consider the σ orbitals in a homonuclear diatomic molecule such as H_2 or N_2. Such a molecule has a symmetry axis $\hat{z}$ joining the two nuclei and a plane of symmetry perpendicular to the axis and half-way between the nuclei. We can form two types of axially symmetric functions by a superposition of identical S functions:

$$\begin{aligned}\phi_\sigma(\boldsymbol{p}) &= V_0^{(1)}(p)\exp(-i\boldsymbol{p}.\boldsymbol{R}_1) \pm V_0^{(2)}(p)\exp(-i\boldsymbol{p}.\boldsymbol{R}_2)\\ &= V_0(p)\{\exp(-i\boldsymbol{p}.\boldsymbol{R}_1)\pm\exp(-i\boldsymbol{p}.\boldsymbol{R}_2)\},\end{aligned} \tag{28}$$

where the plus sign gives a σ_g orbital that is symmetric about the median plane, and the minus sign gives a σ_u orbital that is antisymmetric about this plane, which becomes a nodal plane. The momentum profile or momentum density is given by

$$\rho_\sigma(\boldsymbol{p}) = |\phi_\sigma(\boldsymbol{p})|^2 = 2V_0^2(p)\{1\pm\cos(\boldsymbol{p}.\boldsymbol{R}_{12})\}. \tag{29}$$

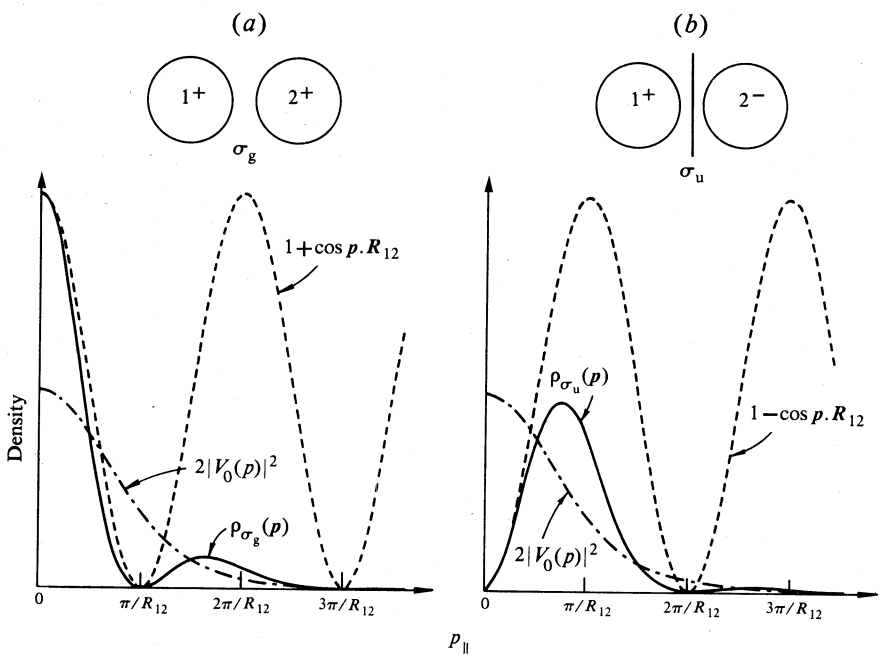

Fig. 2. MO momentum densities $\rho_\sigma(\boldsymbol{p}) = |\phi_\sigma(\boldsymbol{p})|^2$, the summed atomic momentum densities $2|V_0(p)|^2$, and the $1\pm\cos(\boldsymbol{p}.\boldsymbol{R}_{12})$ interference terms plotted along the direction of the internuclear axis $p_\parallel$ for the (*a*) bonding σ_g and (*b*) antibonding σ_u orbitals.

The shape of these various functions along the internuclear axis is shown in Fig. 2. The most obvious effect of the nuclear positions is to introduce nodal planes, perpendicular to the internuclear axis $\hat{z}$, into the momentum profile at momenta spaced by $2\pi/R_{12}$. In the σ_g bonding orbital (Fig. 2*a*) the phase factors result in a concentration,

relative to the atomic momentum, of the momentum density to lower $p_{\|}$ values, where $p_{\|}$ is the momentum parallel to the symmetry axis $\hat{z}$. For the σ_u antibonding orbital (Fig. 2*b*) there is a nodal plane at $p_{\|} = 0$, as required by the symmetry property. There is also a maximum in the momentum density at a position $p_{\|\max} \lesssim \pi/R_{12}$.

The spherically averaged momentum profile for the σ_g orbital is

$$(4\pi)^{-1} \int d\hat{\boldsymbol{p}} \, |\phi_{\sigma_g}(\boldsymbol{p})|^2 = 2V_0^2(p)\left(1 + \frac{\sin(\boldsymbol{p}.\boldsymbol{R}_{12})}{\boldsymbol{p}.\boldsymbol{R}_{12}}\right). \tag{30}$$

This has the character of an atomic s-state profile with superimposed oscillations of period $2\pi/R_{12}$.

For valence orbitals the oscillations are not significant. In H_2 for instance, we have $R_{12} = 1{\cdot}4$ a.u. and the first minimum occurs at $p = 4{\cdot}5$ a.u., where $V_0^2(p)$ is already too small to be observed. For core orbitals, however, $V_0^2(p)$ remains large for $p \gg 2\pi/R_{st}$, and such oscillations should be a prominent feature of the momentum profiles. We have here an excellent example of the 'inverse' (Fourier) relation between momentum and position space. In position space the valence MO have all the information concerning atomic centres, and the core orbitals are essentially atomic in nature. In momentum space the opposite is true, the positions of the atomic centres produce large interference effects in core momentum densities, and have a relatively small effect on the valence orbital momentum densities (except of course on the overall symmetry of the MO).

Instead of maximum density along the $\hat{z}$ axis one also expects a type of symmetry with a node along the $\hat{z}$ axis, and the $\boldsymbol{P}$ functions can be used to describe this. For example, P_x has a nodal plane yz through the origin, being positive for positive x and negative for negative x. A superposition of identical P_x functions gives rise to π_x MO. Superposition of P_y functions produces π_y MO, which are identical to π_x orbitals but rotated about $\hat{z}$ by 90°. Superposition of P_z orbitals produces σ orbitals, which are symmetric about the $\hat{z}$ axis. We can therefore add P_z functions to S functions to give more freedom in describing the shape of σ orbitals. Similarly, we can add symmetry functions derived from higher order spherical harmonics (D, F, etc.) to give us more flexibility in describing the shape of the orbitals.

5. Cross Section for Atoms

Hydrogen

The simplest case is atomic hydrogen where the overlap between the initial ground state and the ion state (free proton) is simply $\phi_{1s}(p)$, and

$$\sigma_H = (2\pi)^4 f_{ee}(p_A p_B/p_0)|\, \phi_{1s}(p)\,|^2 . \tag{31}$$

The ground state wavefunction for a one electron system is given by (in a.u.)

$$\phi_{1s}(p) = \{(2Z)^{3/2}/\pi\}\{1/(p^2+Z^2)^2\}. \tag{32}$$

Therefore, for atomic hydrogen the electron momentum probability distribution should be given simply by

$$|\,\phi_{1s}(p)\,|^2 = (2^3/\pi^2)(1+p^2)^{-4}. \tag{33}$$

If non-coplanar symmetric kinematics are used the shape of the (e, 2e) cross section should be this momentum probability distribution.

The momentum distributions obtained by Lohmann and Weigold (1981) at 400, 800 and 1200 eV are shown in Fig. 3. The momentum distributions normalized to unity are independent of energy and in excellent agreement with the solution (33) to Schrödinger's equation. The data of Lohmann and Weigold provide a direct experimental demonstration of the interpretation of wavefunctions as probability amplitudes in the simplest case, namely atomic hydrogen.

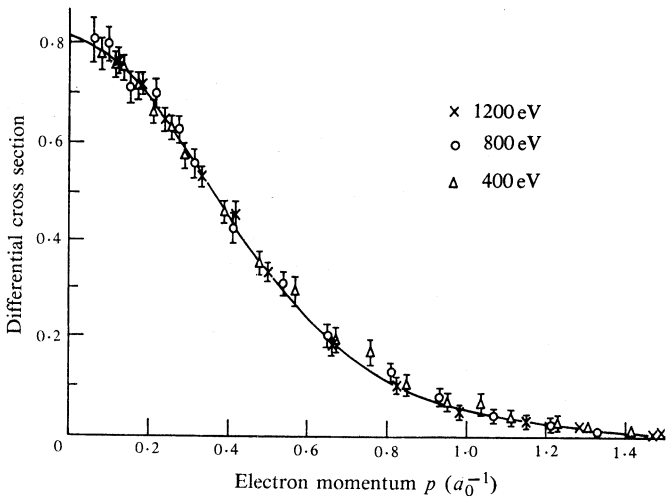

Fig. 3. Non-coplanar symmetric (e, 2e) differential cross section for atomic hydrogen at 400, 800 and 1200 eV (Lohmann and Weigold 1981) compared with the square of the exact momentum space wavefunction $|\phi_{1s}(p)|^2$ (curve) of equation (33).

Helium

Without the interaction term $1/r_{12}$ between the two electrons in the helium atom, the ground state eigenfunction would be simply the product of two hydrogenic ground state wavefunctions with charge $Z = 2$:

$$\Psi_0^N(r_1, r_2) = \psi_0(r_1)\psi_0(r_2) = (Z^3/\pi)\exp\{-Z(r_1+r_2)\}, \tag{34}$$

and the overlap of this with the helium ion ground state $\psi_0(r_2)$ would be simply

$$\langle \boldsymbol{p}\Psi_F^{N-1} \mid \Psi_0^N\rangle = \int \mathrm{d}^3p_1\, \phi_{1s}^*(p_1)\phi_{1s}(p_1)\phi_{1s}(p)$$
$$= \{(2Z)^{3/2}/\pi\}\{1/(p^2+Z^2)^2\}. \tag{35}$$

In this approximation no other ion states could be excited since they are all orthogonal to $\psi_0(r)$. In the HF approximation for helium, the overlap would still be of the form (35) but the integral over the coordinates of electron 1 would not be orthonormal since there would be different self-consistent fields in the atom and ion. Thus, excitation of higher s states in the ion would be possible, although the integral of $\phi_{ns}^*(p_1)\phi_{1s}(p_1)$ would be small for $n \neq 1$. Further, with a correlated helium ground state wavefunction, which contains $(\phi_{2p})^2$ configurations, it would be possible to excite the 2p ion eigenstate as well as the 2s.

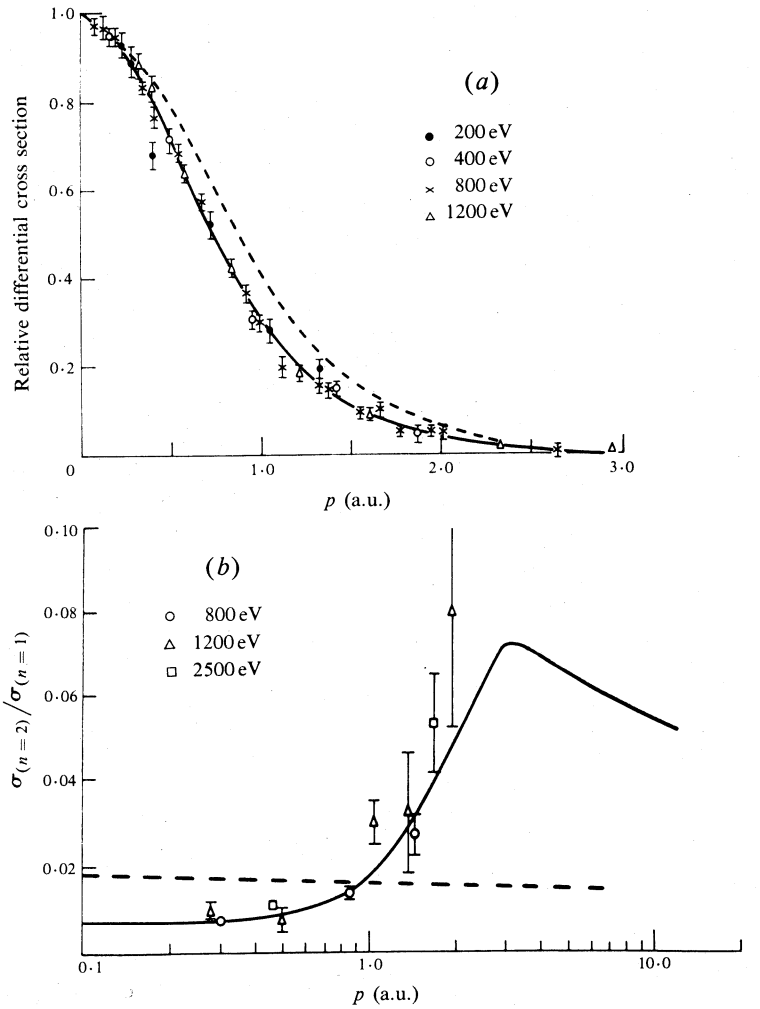

Fig. 4. (*a*) Non-coplanar symmetric (e, 2e) cross section for the He ground state transition at four different total energies (Weigold and McCarthy 1978). The solid and dashed curves are the squares of the 1s momentum space wavefunctions using respectively a HF wavefunction and a hydrogenic wavefunction with $Z = 2$. Theory and data have been normalized to unity at $p = 0$. (*b*) Ratio of the cross section for exciting the $n = 2$ levels of He^+ to the ground state 1s cross section plotted as a function of p. The data were taken at three energies (Dixon *et al.* 1976). The dashed line is the PWIA result using the HF wavefunction for He and the solid curve is the result obtained using an accurate correlated He ground state wavefunction.

Fig. 4*a* shows some non-coplanar symmetric (e, 2e) cross section measurements for the ground state transition in helium over a range of total energies from 200 to 1200 eV plotted as a function of the momentum p (Weigold and McCarthy 1978). The shape of the cross sections, which have been normalized to unity at $p = 0$, is independent of energy. This is an important confirmation of the reaction model, since in this geometry the shape of the cross section is given directly by the square of the overlap function. The dashed curve is the shape given by the overlap function (35) using the value $Z = 2$. The excellent agreement between the measured cross

sections and the HF 1s orbital momentum distribution (solid curve) shows that the independent particle model of the atom is a very good approximation in the case of helium.

Correlated ground state wavefunctions give essentially the same momentum distribution as the HF wavefunction for the ground state transition, but quite different distributions for transitions to the $n = 2$ (2s, 2p) eigenstates of the ion. Fig. 4*b* shows the experimental results of Dixon *et al.* (1976). The very small measured cross sections to the excited states are in excellent agreement with calculations using an accurate correlated helium ground state wavefunction in the overlap amplitude (solid curve), and in marked disagreement with the HF calculation (dashed line). The excitation of the $n = 2$ states is a sensitive test of ground state correlations.

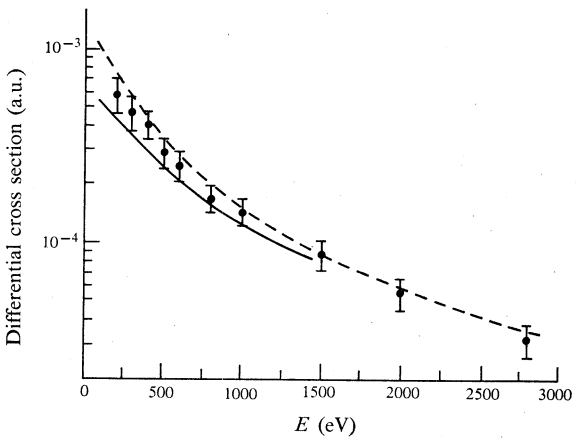

Fig. 5. Absolute symmetric (e, 2e) cross sections for He at $\theta = 45°$, $\phi = 0°$ plotted as a function of the total energy E $(=E_0-\varepsilon)$ (van Wingerden *et al.* 1979). The dashed and solid curves are the PWIA and DWIA calculations respectively using a HF He ground state wavefunction.

Most (e, 2e) differential cross section measurements are not absolute but only relative due to the difficulty of making absolute measurements in an electron impact ionizing experiment with gas targets. However, for helium accurate absolute measurements have been made in the symmetric geometry ($\theta = 45°$, $\phi = 0°$) by van Wingerden *et al.* (1979). Their results are shown in Fig. 5 compared with a PWIA calculation (dashed curve) using a HF wavefunction for the helium ground state. They are also compared with the results (solid curve) of a distorted wave impulse approximation (DWIA) calculation (Dixon *et al.* 1978; Fuss *et al.* 1978), which allows for distortion and absorption in the incident and outgoing electron waves. At sufficiently high energies the DWIA should merge into the PWIA result. Agreement between the calculated and measured absolute cross sections is excellent.

Krypton

Before going on to molecules it is interesting to consider the results for a heavier noble gas such as krypton, whose valence ground state HF configuration is $(\text{core})(4s)^2(4p)^6$.

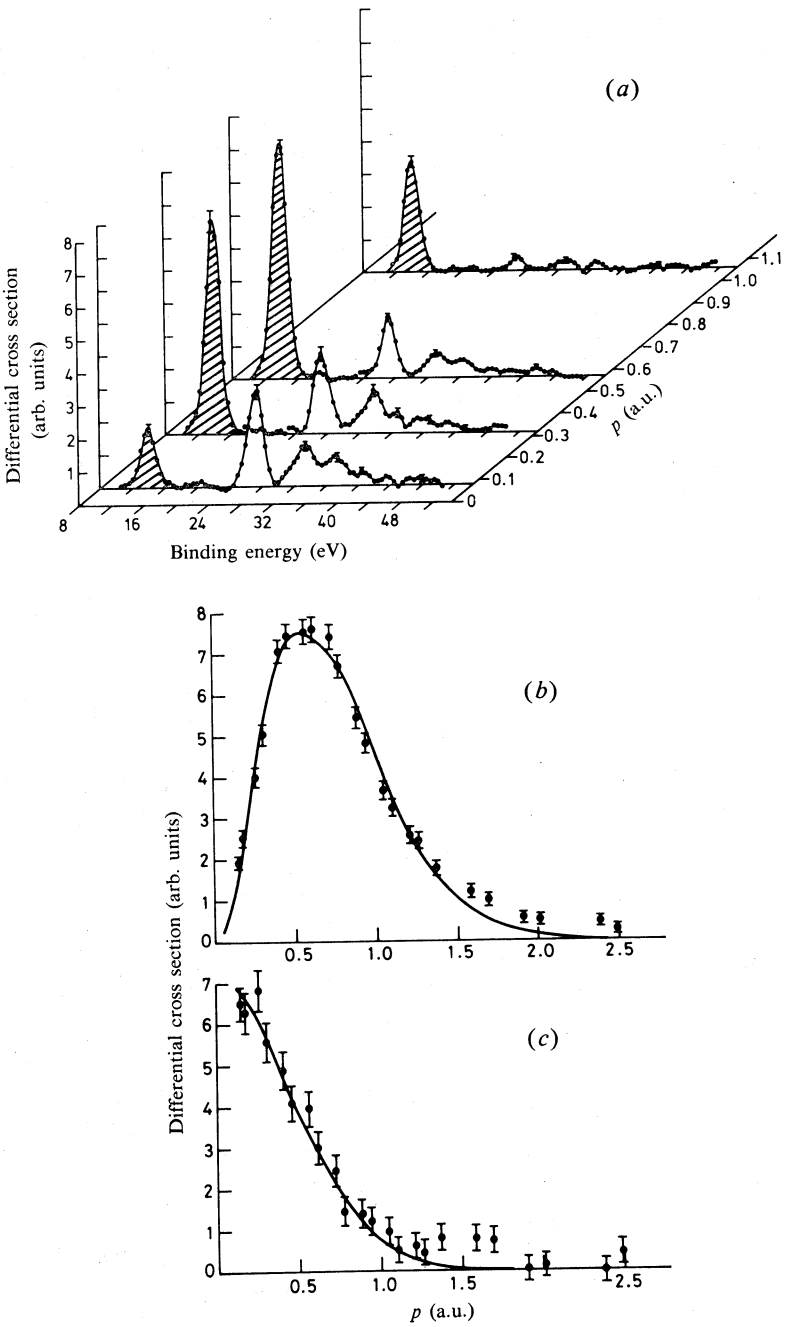

Fig. 6. Non-coplanar symmetric (e, 2e) cross sections for krypton at 1200 eV: separation energy spectra (*a*) plotted as a function of the out-of-plane azimuthal angle ϕ (i.e. momentum p); angular correlations for transitions to (*b*) the ground state (4p) and (*c*) the excited states (4s) plotted as a function of momentum p and compared with calculated HF momentum distributions (solid curves).

In the (e, 2e) valence separation energy spectrum of krypton we would therefore expect to see two peaks, one resulting from the removal of a 4p electron (leading to the ground state of the ion since the 4p electrons are least bound) and a similar peak resulting from the removal of a 4s electron. For each peak one should obtain a momentum distribution given by $|\phi_{4p}|^2$ and $|\phi_{4s}|^2$ respectively. The 4s distribution for krypton is similar in shape to the 1s momentum distribution in helium and hydrogen, peaking at $p = 0$ and decreasing as p increases. The calculated 4p momentum distribution is however quite different. It is zero at $p = 0$, has a maximum at $p \approx 0{\cdot}6$ a.u. and then decreases to zero as p increases.

In fact the measured valence separation energy spectra of krypton show much more structure than the two expected peaks. Fig. 6*a* shows separation energy spectra taken at a number of azimuthal angles ϕ (i.e. momentum p) by Fuss *et al.* (1981). The lowest energy peak resulting from the transition to the ground state of the ion has a low intensity at small p and a maximum at $p \approx 0{\cdot}6$ a.u., just what would be expected on the basis of the knockout of a 4p electron. Indeed, the momentum distribution for this peak is in excellent agreement with the calculated HF 4p momentum distribution (Fig. 6*b*).

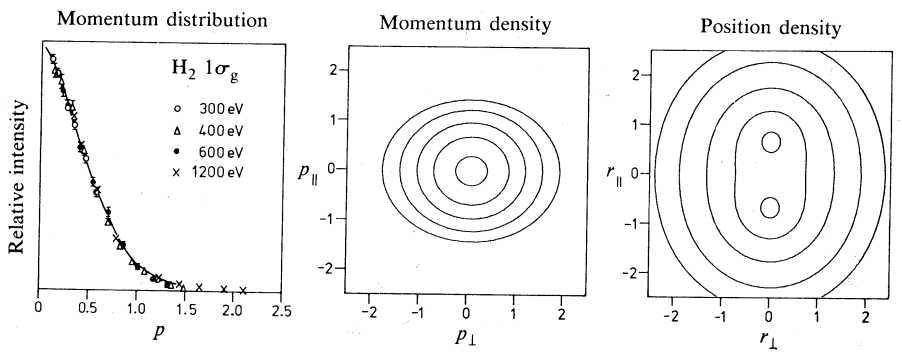

Fig. 7. Momentum distributions and momentum and position density maps for the $1\sigma_g$ orbital of H_2 using the MO wavefunctions of Snyder and Basch (1972). The data are from Dey *et al.* (1975). Contours are at 1%, 3%, 10%, 30% and 80% of the maximum intensity. The scales are in a.u.

All the peaks at higher separation energies have their maximum intensity at $p \approx 0$ and must therefore belong to the 4s orbital. The momentum distributions for these peaks agree very well with the calculated HF 4s orbital momentum distribution (Fig. 6*c* shows an example). This splitting of the 4s orbital among a number of ion states must be due to a breakdown of the independent particle picture for either the ground state of krypton, the krypton ion, or both. The fact that the shape of the momentum distributions of the peaks is well described by the HF orbital momentum distributions suggests that the independent particle model is a good approximation for the ground state of krypton. Detailed calculations (Fuss *et al.* 1981) confirm this and show that the breakdown does indeed occur in the ion eigenstates. The ion eigenstates can only be described by wavefunctions which explicitly include electron correlation effects.

The fact that we have the 4s (e, 2e) momentum profile for each of the ion eigenstates into which the 4s independent particle state splits shows that the reaction selects a component in each correlated wavefunction which is just the 4s independent

particle state. In fact detailed analysis shows that the differential cross section for exciting the eigenstate is proportional to the probability of finding the relevant independent particle state as a component of the correlated wavefunction (see equation 19 and McCarthy and Weigold 1976). Thus the concept of an orbital is extended from the independent particle model to the actual situation.

6. Cross Section for Molecules

Hydrogen

The simplest molecule is H_2 with a $(1\sigma_g)^2$ independent particle MO ground state configuration. Since the ion ground state is a $1\sigma_g$ MO, the overlap function leads to

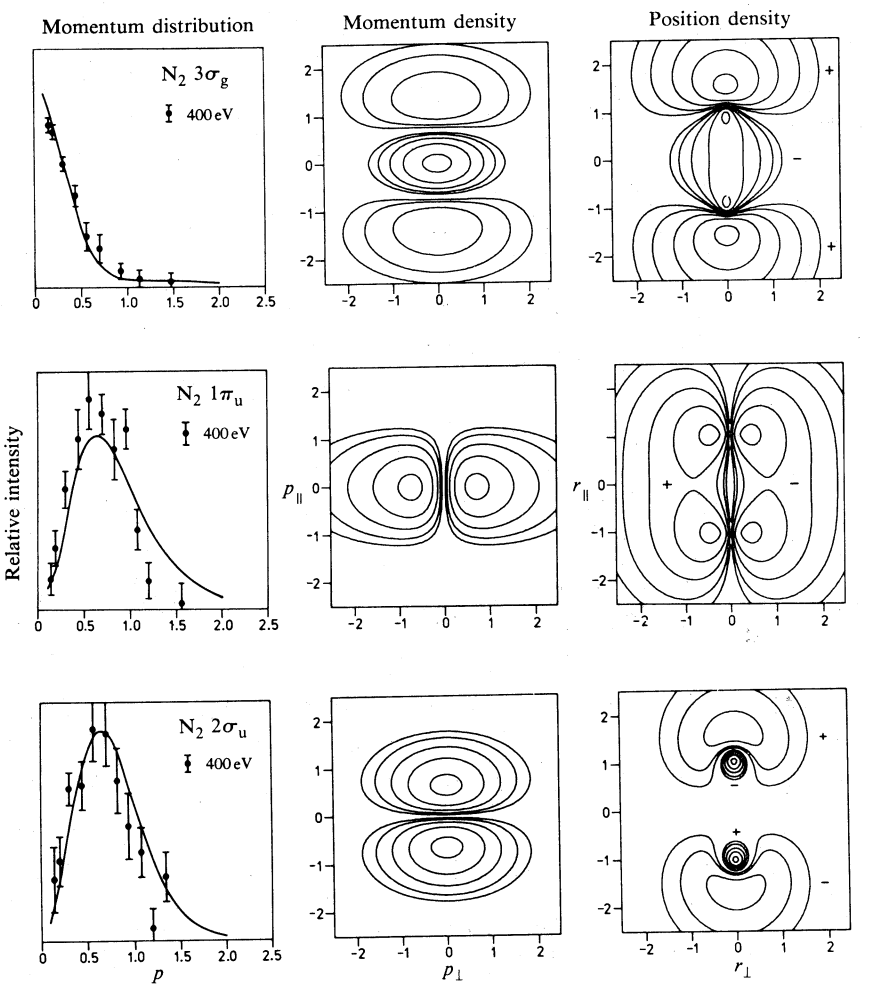

(*a*)

Fig. 8. Momentum distributions and momentum and position density maps (Cook 1982) for (*a*) the outer valence orbitals and (*b*) the inner valence $2\sigma_g$ and core orbitals of N_2, using the MO wavefunctions of Snyder and Basch (1972). The data are from Weigold *et al.* (1977). The sign of the position space wavefunction is indicated. Contours are at 1%, 3%, 10%, 30% and 80% of the maximum intensity. The scales are in a.u.

a $1\sigma_g$ MO momentum distribution. The momentum and position density maps (Cook 1982) calculated using the wavefunctions of Snyder and Basch (1972) are shown in Fig. 7. As expected the σ_g density is essentially an s-type stretched along the $\hat{z}$ axis in position space and contracted along the $\hat{z}$ axis in momentum space. The spherically averaged momentum distribution is in excellent agreement with the measured non-coplanar (e, 2e) cross section (Dey *et al.* 1975).

As in the case of helium, the cross section leading to the excited states of H_2^+ provides a sensitive test of ground state correlations in H_2 (Dey *et al.* 1975).

Nitrogen

The independent particle electronic configuration for N_2 is

$$(1\sigma_g)^2(1\sigma_u)^2(2\sigma_g)^2(2\sigma_u)^2(1\pi_u)^4(3\sigma_g)^2 .$$

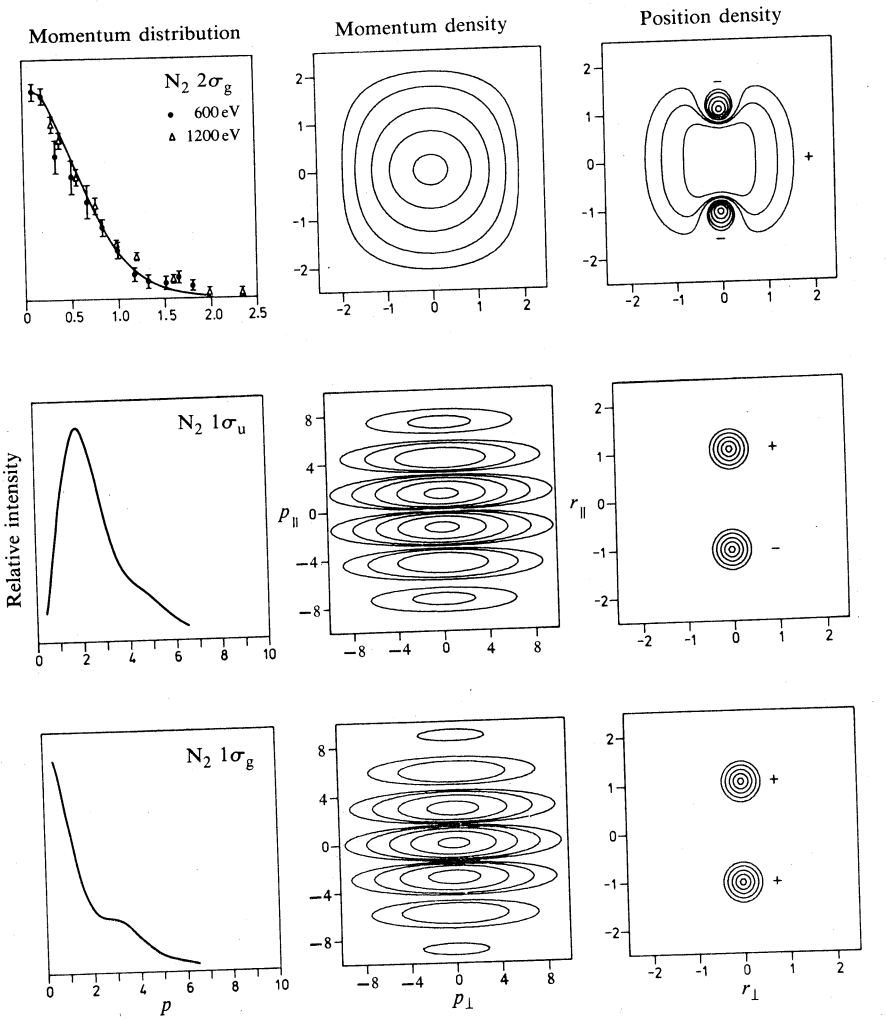

(*b*)

Fig. 8*b* [*see caption opposite page*]

Calculated position and momentum density maps (Cook 1982) are shown in Fig. 8, which also shows spherically averaged momentum distributions for the valence orbitals compared with measured momentum profiles (Weigold *et al.* 1977). The MO wavefunctions used are again those of Snyder and Basch (1972). The interference effect due to the nuclear positions is most evident in the momentum density maps for the two core orbitals $1\sigma_g$ and $1\sigma_u$. In momentum space the innermost valence $2\sigma_g$ and the $2\sigma_u$ orbitals are respectively similar in character to the $1\sigma_g$ and the unoccupied $1\sigma_u$ orbitals in H_2.

The absence of density in the charge density map along the $r_{\|} = 0$ plane in the $2\sigma_u$ orbital (Fig. 8*a*) indicates the strong antibonding character of this orbital. This nodal plane must, since symmetry is conserved, appear in the momentum density maps. The π_u orbital on the other hand is bonding, which in momentum space is evidenced by a contraction of the momentum density in the $p_{\|}$ direction.

The outermost $3\sigma_g$ orbital is non-bonding. The two nodal planes at $p_{\|} = \pm 0{\cdot}75$ a.u. lead to a narrow spherically averaged momentum distribution. The small amount of density in the lobes at large $p_{\|}$ gives rise to a very small spherically averaged density at large p.

Hydrogen Halides

The hydrogen halides are isoelectronic with the noble gases, and their electronic ground state configurations can be written in the independent particle MO model as

$$\text{core}(ns\sigma)^2(np\sigma)^2(np\pi)^4\,;{}^1\Sigma^+ .$$

The inner valence σ orbital in the LCAO approximation is mainly composed of the heavy atom ns orbital and the hydrogen 1s orbital. Similarly the $np\sigma$ and $np\pi$ orbitals in the LCAO picture are mainly due respectively to the P_z and $P_{x,y}$ orbitals of the heavy atom with a function on the H atom. Thus, the two outermost valence orbitals can be regarded as arising from a splitting of the $(np)^6$ shell of the isoelectronic noble gas.

The valence separation energy spectra at two values of ϕ (i.e. momentum p) are shown in Fig. 9. The data for HF and HCl are from Brion *et al.* (1980) and for HBr and HI from Brion *et al.* (1982). The outer valence $np\pi$ and $np\sigma$ transitions have a small cross section at $\phi = 0°$ ($p \approx 0{\cdot}07$ a.u.), whereas the inner valence $ns\sigma$ transition peaks at $\phi = 0°$. For the HF molecule only the three peaks expected from the H–F model are seen. In this it is similar to its isoelectronic atomic counterpart, neon (McCarthy and Weigold 1976). For HCl, HBr and HI the outer valence states remain unsplit, but the $ns\sigma$ transition is seriously split among many ion states. This is again similar to the significant splitting observed in the ns transitions in Ar, Kr and Xe (McCarthy and Weigold 1976). In fact the pole strengths or spectroscopic factors for the 'main' inner valence transition in Ne, Ar, Kr and Xe are found to be 0·96, 0·54, 0·45 and 0·32 respectively (compared with the independent particle value of 1). In comparison, the pole strengths for the 'main' $ns\sigma$ transition in HF, HCl, HBr and HI are found to be approximately 1, 0·51, 0·42 and 0·37 respectively.

Brion *et al.* (1980, 1982) compared their results with several one particle Green function calculations using the two-particle–hole Tamm–Dancoff approximation.

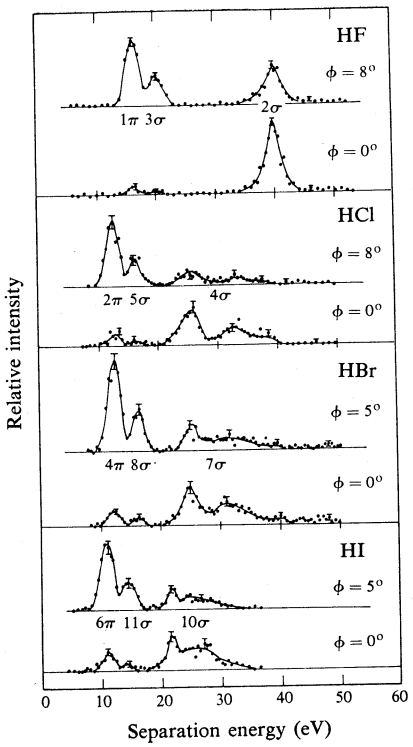

Fig. 9. Non-coplanar symmetric separation energy spectra at 1200 eV for four hydrogen halides in the valence region at the out-of-plane azimuthal angles ϕ indicated (Brion *et al.* 1980, 1982).

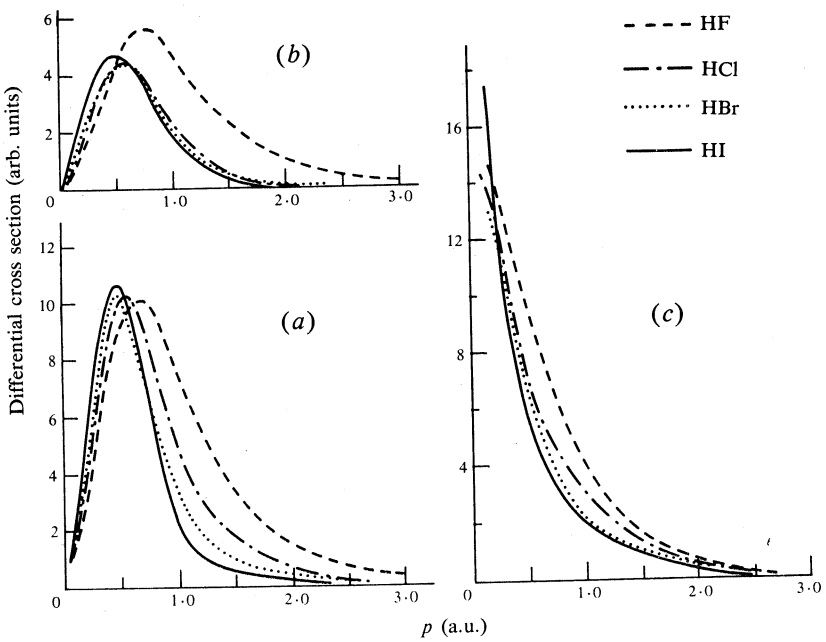

Fig. 10. Measured non-coplanar symmetric differential cross sections for the (*a*) $np\pi$, (*b*) $np\sigma$ and (*c*) $ns\sigma$ valence orbitals of the hydrogen halides (Brion *et al.* 1980, 1982). The momentum profiles have been normalized to give approximately the same peak heights for the outer valence $np\pi$ orbital.

Although this approximation allows for correlation in the initial and final states as well as relaxation, the agreement between the calculated and measured splitting of the inner valence $ns\sigma$ orbitals is only qualitative.

The observed momentum distributions for the hydrogen halides are summarized in Fig. 10. The cross sections have all been plotted so that the peak heights of the π orbital momentum distributions in Fig. 10*a* are approximately equal, the other relative normalizations being preserved. The periodic trends are obvious. As we proceed from HF to HI, the peaks in the momentum profiles of the two outer valence orbitals move to lower p and the full width at half maximum of the profiles for the $np\pi$ and $np\sigma$ orbitals gets significantly smaller. The tendency for the low momentum components to become more significant in the probability distribution with increasing charge number is also evident in the inner valence $ns\sigma$ orbital momentum distribution (Fig. 10*c*). This implies that in coordinate space the valence orbitals of HBr and HI are quite diffuse, whereas the outer orbitals of HF are much more localized at the atomic sites. The valence orbital momentum distributions for HF are very different from those for HCl, HBr and HI, which are quite similar to each other. Chemically, HF is also very different from the other three hydrogen halides. For instance, HF is significantly hydrogen bonded whereas the others are not. This chemical difference must be reflected in differences in the momentum distributions.

Brion *et al.* (1980, 1982) also found that in order to fit the observed momentum distributions it is often necessary to go beyond quite sophisticated MO calculations. The best fits are obtained with the use of the generalized overlap amplitudes obtained from the Green function calculations. In the case of HF they found quite serious disagreement between the MO π orbital momentum distributions and those observed.

7. Summary

Electron coincidence spectroscopy in the non-coplanar symmetric geometry provides us with a powerful tool for investigating the electronic structure of atoms and molecules. It provides separation energy spectra at a number of out-of-plane azimuthal angles ϕ, i.e. at a number of bound electron momenta p. These spectra yield direct information on the symmetry and energies of the valence orbitals as well as on the characteristic orbital giving rise to 'satellite' transitions. At times such satellite transitions can dominate the main transition, indicating an almost complete breakdown of the independent particle model. The pole strength or spectroscopic factor, which is the probability of finding a single hole configuration in the many body wavefunction for the ion state, can be directly measured. It is possible to measure ground state correlations as well as final state correlations and to separate the two.

Of major importance, however, is that the technique allows the direct measurement of momentum densities for individual orbitals. These have, until now, been restricted to spherically averaged momentum densities, but with the use of oriented targets (for example, crystals and molecules absorbed on surfaces) it should be possible to measure directional momentum densities. Much work, however, remains to be done in obtaining direct 'chemical' understanding from momentum space measurements. We are used to thinking in position space but not in momentum space. Various techniques are being developed to bridge the gap between momentum space and configuration space pictures of chemical bonding (Coplan *et al.* 1982; Cook 1982).

Finally, it should be pointed out that (e, 2e) spectroscopy is particularly sensitive to the valence and the low momentum region. Since low momentum means on the

average the outer region of the molecule, this is obviously the chemically interesting region.

Acknowledgments

Much of the work reported here was supported by the Australian Research Grant Scheme. I am grateful to I. E. McCarthy, C. E. Brion, J. P. D. Cook and A. Minchinton for many fruitful discussions.

References

Brion, C. E., Hood, S. T., Suzuki, I. H., Weigold, E., and Williams, G. R. J. (1980). *J. Electron Spectrosc. Relat. Phenom.* **21**, 71.
Brion, C. E., *et al.* (1982). *J. Electron Spectrosc. Relat. Phenom.* **27**, 83.
Clementi, E., and Roetti, R. (1974). *At. Data Nucl. Data Tables* **14**, 177.
Cook, J. P. D. (1982). *In* 'Momentum Distributions in Atomic, Molecular and Nuclear Systems' (Ed. E. Weigold), A.I.P. Conference Proceedings No. 86, p. 278 (A.I.P. Press: New York).
Coplan, M. A., Tossell, J. A., and Moore, J. H. (1982). *In* 'Momentum Distributions in Atomic, Molecular and Nuclear Systems' (Ed. E. Weigold), A.I.P. Conference Proceedings No. 86, p. 82 (A.I.P. Press: New York).
Dey, S., McCarthy, I. E., Teubner, P. J. O., and Weigold, E. (1975). *Phys. Rev. Lett.* **34**, 782.
Dixon, A. J., Dey, S., McCarthy, I. E., Weigold, E., and Williams, G. R. J. (1977). *Chem. Phys.* **21**, 81.
Dixon, A. J., McCarthy, I. E., Noble, C. J., and Weigold, E. (1978). *Phys. Rev.* A **17**, 597.
Dixon, A. J., McCarthy, I. E., and Weigold, E. (1976). *J. Phys.* B **9**, L195.
Duncanson, W. E., and Coulson, C. A. (1941). *Proc. Cambridge Philos. Soc.* **37**, 406.
Fuss, I., Glass, R., McCarthy, I. E., Minchinton, A., and Weigold, E. (1981). *J. Phys.* B **14**, 3277.
Fuss, I., McCarthy, I. E., Noble, C. J., and Weigold, E. (1978). *Phys. Rev.* A **17**, 604.
Lohmann, B., and Weigold, E. (1981). *Phys. Lett.* A **86**, 139.
McCarthy, I. E., and Weigold, E. (1976). *Phys. Rev.* C **27**, 275.
Snyder, L. C., and Basch, H. (1972). 'Molecular Wave Functions and Properties' (Wiley: New York).
van Wingerden, B., *et al.* (1979). *J. Phys.* B **12**, L627.
Weigold, E. (1981). *Nucl. Phys.* A **353**, 327.
Weigold, E., Dey, S., Dixon, A. J., McCarthy, I. E., Lassey, K. R., and Teubner, P. J. O. (1977). *J. Electron Spectrosc. Relat. Phenom.* **10**, 177.
Weigold, E., and McCarthy, I. E. (1978). *Adv. Atom. Mol. Phys.* **14**, 127.
Williams, G. R. J., McCarthy, I. E., and Weigold, E. (1977). *Chem. Phys.* **22**, 281.

Manuscript received 21 June, accepted 13 August 1982